

FABRICATION AND CHARACTERIZATION OF MICROCRYSTALLINE CELLULOSE FROM SENGON WOOD SAWDUST

INTAN MARTHA CAHYANI,^{*,**} ENDANG LUKITANINGSIH,^{***}
ADHYATMIKA ADHYATMIKA^{****} and TEUKU NANDA SAIFULLAH SULAIMAN^{****}

^{*}*Doctoral Program of Pharmaceutical Science, Faculty of Pharmacy,
Universtias Gadjah Mada, Indonesia*

^{**}*STIFAR “Yayasan Pharmasi”, Letjend Sarwo Edie Wibowo KM 1, Semarang, Indonesia*

^{***}*Department of Pharmaceutical Chemistry, Faculty of Pharmacy,
Universtias Gadjah Mada, Indonesia*

^{****}*Department of Pharmaceutics, Faculty of Pharmacy, Universtias Gadjah Mada, Indonesia*

✉ *Corresponding author: T. N. S. Sulaiman, tn_saifullah@ugm.ac.id*

Received April 21, 2024

Sengon wood sawdust is a wood industry waste the quantity of which is increasing because of the high market demand of the wood. This condition demands innovation in waste processing. Microcrystalline cellulose is pure cellulose obtained from the hydrolysis of α -cellulose. This research aims to fabricate and characterize microcrystalline cellulose from Sengon wood sawdust. The initial stage was carried out to break lignocellulose bonds through the delignification process using 2% NaOH, followed by hydrolysis of α -cellulose with 4N HCl (1:40) at 80 °C. This acid treatment aims to obtain a crystalline form of cellulose by removing the amorphous part. SEM micrographs show a smooth surface with few holes and spherical fibers. XRD analysis revealed the cellulose type I structure of MCC with a crystallinity index of 33.8% due to acid hydrolysis treatment. Chemical treatment causes the loss of the hemicelluloses and lignin, as confirmed from the FT-IR analysis results, and higher thermal stability of microcrystalline cellulose, as found by the DSC analysis.

Keywords: characterization, fabrication, microcrystalline cellulose, Sengon wood sawdust, waste treatment

INTRODUCTION

Sengon is a woody plant that is widely cultivated in Indonesia.¹ Its wood has an attractive texture, color, and fiber. Therefore, it is in great demand as raw material for furniture or tools, and is used by the wood plastic composite (WPC) industry. The high market demand for Sengon wood products also has an impact on the large amount of waste produced by the wood industry. Managing large quantities of waste faces several challenges. In recent decades, significant research attention has been focused on products derived from processing plant fibers, encompassing both wood and non-wood sources, such as Parawood sawdust,² bamboo sticks,³ coffee and rice husk,⁴ date seeds,⁵ and tea waste.⁶ Plant fibers have properties that are widely used by industry due to the presence of cellulose as the main component.⁷ The cellulose content in Sengon wood is relatively high (52.23%),⁸ with a high potential to

be processed into various products as an effort to increase the useful and economic value of wood industry waste.

Cellulose is a linear, unbranched homopolysaccharide formed from repeating β -(1 \rightarrow 4) linked D-glucose units.⁵ Cellulose can be processed into various types of particles, including cellulose nanocrystals,⁹ cellulose nano whiskers,¹⁰ and microcrystalline cellulose.¹¹ Microcrystalline cellulose has a wide use in the industry, including in producing tablets,¹² absorbents,^{13,14} and biocomposite films.¹⁵

Microcrystalline cellulose is one of the products resulting from processing cellulose by acid hydrolysis.¹⁶ Other methods that can also be used to isolate microcrystalline cellulose include steam explosion, extrusion, or radiation-enzymatic processes. However, the acid hydrolysis method is often chosen due to its

simple procedure, fast reaction rate, and mild conditions.⁷ In order to optimize the quality of the microcrystalline cellulose produced, strong acids, such as hydrochloric acid, sulfuric acid or nitric acid are often used.¹⁷ The effectiveness of acid hydrolysis in making microcrystalline cellulose has been widely reported, including the use of sulfuric acid in the hydrolysis of coffee husk,⁴ a mixture of strong acids on giant reed,¹⁸ and hydrochloric acid in *Ensete glaucum*.²⁰ Hydrochloric acid has been proven to be more effective than sulfuric acid in the hydrolysis process of woody plant fiber cellulose at an optimum treatment of 1:15, temperature of 80 °C for 2 h, producing 76.89%-77.67% microcrystalline cellulose.² Therefore, in this research, hydrochloric acid was used in the hydrolysis process.

This research aims to investigate the use of Sengon wood sawdust waste as a renewable resource to produce microcrystalline cellulose. Producing microcrystalline cellulose consists of three stages, namely delignification with sodium hydroxide (NaOH), acid hydrolysis with hydrochloric acid (HCl), and bleaching with sodium hypochlorite (NaOCl). The ultrasonic delignification stage of Sengon wood sawdust has been reported to produce 77.96% α -cellulose.²¹ Based on this description, further research regarding the acid hydrolysis process to obtain microcrystalline cellulose is required to be conducted. The resulting Sengon wood sawdust microcrystalline cellulose was characterized in terms of functional groups, using Fourier transform infrared spectroscopy (FTIR), cellulose morphology using a scanning electron microscope (SEM), and degree of crystallinity using an X-ray diffractometer (XRD). Differential scanning calorimetry (DSC) was used to analyze the thermal properties of the obtained microcrystalline cellulose.

EXPERIMENTAL

The sample of Sengon wood sawdust (SWS) was obtained as a by-product from CV Cahaya Abadi Chip (located in Kaliwungu-Kendal). It originated from the sanding process of Sengon wood pith using a 250-grit machine, and served as the primary material for the study. Sodium hydroxide (NaOH), hydrochloric acid (HCl), sodium hypochlorite (NaOCl) and distilled water were used in the experiments, and Avicel PH 102 was used as commercial standard.

Fabrication of microcrystalline cellulose

SWS was processed in two stages, first, the delignification process used NaOH solution under the optimal conditions defined earlier²¹ to obtain Sengon wood sawdust cellulose (SWS-C). The second stage was hydrolysis of SWS-C with 4N HCL at 80 °C for 4 h with constant stirring in the ratio (1:40) pulp to liquor. The hydrolysis product was then filtered at room temperature and washed repeatedly with distilled water until the pH was neutral. MCC obtained from SWS-C pulp was then bleached with 10% NaOCl at 75 °C for 1 h and rinsed again until the pH was neutral, then dried and ground at 60 mesh to obtain Sengon wood sawdust microcrystalline cellulose (SWS-MCC).²²

Chemical composition of SWS-MCC

The chemical composition of SWS-MCC and commercial MCC was determined using the Chesson-Data method.²³

Structural characterization of SWS-MCC

FT-IR analysis

The infrared spectra of the dried SWS-MCC samples were recorded using an IR instrument (Agilent Technologies Cary 630 FT-IR); and 34 scans were collected in the wavelength range of 500-4000 cm^{-1} . The position of significant transmittance peaks was determined using the "Find peak" tool provided by the Agilent Microlab Expert software. The spectrum was obtained at a temperature of 25 °C between 750-3750 cm^{-1} .

Morphological analysis (SEM)

The morphology of Sengon wood sawdust microcrystalline cellulose was observed using a JEOL JSM-6510LA Scanning Electron Microscope, with an Auto Coater (JEOL JEC-3000FC), which has a magnification specification of 10-300.000x and a resolution of 1-10 nm.

X-ray diffraction (XRD) analysis

A D8 Advance X-ray diffractometer was used to determine the crystallinity of the prepared Sengon wood sawdust microcrystalline cellulose. The diffraction pattern was recorded in 2θ (10-80). The resulting spectrum results were then processed and analyzed to verify the presence of cellulose in the sample and determine crystallinity (CrI) using Equation (1):

$$\text{CrI (\%)} = (I_{002} - I_{am}) / I_{002} \times 100 \quad (1)$$

where I_{002} is the maximum intensity in the crystalline region ($2\theta = 22.5^\circ$) and I_{am} is the lowest intensity in the amorphous region ($2\theta = 18.5^\circ$).⁶

Thermal analysis

Thermal analysis of microcrystalline cellulose was carried out using differential scanning calorimetry (DSC-60 Shimadzu) in the temperature range of 30–600 °C, using a standard cooling chamber, at a liquid nitrogen flow rate of 10 mL/second (measuring range ± 150 mW).

RESULTS AND DISCUSSION

Chemical composition of SWS-MCC

The chemical composition of SWS-MCC and Avicel as a commercial standard is presented comparatively in Table 1. It can be seen that the cellulose concentration of SWS-MCC (85.01%) is not significantly different from that of Avicel (80.81%), as are the concentrations of hemicelluloses and lignin. This shows that chemical treatment, both delignification and hydrolysis, can reduce hemicelluloses and lignin. From these two treatment stages, it was proven that acid hydrolysis had a greater effect on increasing the cellulose content in SWS,²¹ so acid hydrolysis had a more significant effect compared to the alkali delignification treatment. This result is greater when compared to the results for other plant fibers^{2,18} and there are also comparable ones.²⁴ The bleaching process is also known to influence the purification of cellulose fibers. This is associated with differences in pigmentation of the remaining lignin fraction. Overall, it is effective in removing non-cellulosic components, such as lignin, hemicelluloses, pectin and waxes, as previously reported.^{4,25}

Structural characterization of SWS-MCC

Chemical functionality (FT-IR)

Cellulose molecules consist of the elements C, O, and H with the chemical formula $(C_6H_{10}O_5)_n$ and very strong hydrogen bonds.²⁶ The FTIR

spectrum of SWS-MCC is shown in Figure 1. Absorption bands in the areas around 3330 cm^{-1} , 2900 cm^{-1} , 1430 cm^{-1} , and 890 cm^{-1} are visible, all of the spectra being characteristic of native cellulose.^{27,28,29} The broad peak in the intense absorption band at 3333 cm^{-1} indicates the O-H group stretching in cellulose. The region of 2893 cm^{-1} is considered to be due to the stretching vibration of aliphatic saturated C-H bonds present in cellulose.^{30,27,31} The absorption of water by cellulose, which causes cellulose-water interactions in the fiber, is presented with a band at 1633 cm^{-1} , as mentioned in previous research.³² The absorption peak at 1432 cm^{-1} was identified as the cellulose “crystallinity band” by the presence of $-CH_2$ symmetric bending vibration groups.^{33,34} The presence of C-O stretching groups in cellulose was indicated by the appearance of a peak at 1153 cm^{-1} . The band at 1022 cm^{-1} shows skeletal stretching vibration of the C-O-C pyranose ring of cellulose.^{30,34,27} The peak seen at 891 cm^{-1} indicates the presence of β -glycosidic bonds in the cellulose functional group.³⁵ SWS-MCC has the same functional groups as Avicel. This shows that the procedure carried out in this study can produce MCC with similar composition to that of corresponding commercially available products. The peak visible in the 1700 cm^{-1} region shows the presence of acetyl groups and hemicellulose esters or carboxy groups in lignin, the peaks being present only in the SWS spectrum, whereas in SWS-MCC and Avicel no peaks are visible in this area. The SWS-MCC and Avicel spectra do not show any clusters of C=C (stretching) of the aromatic chains in lignin, which indicates that lignin and hemicelluloses were partially eliminated,³⁶ through the delignification and hydrolysis processes that have been carried out.

Table 1
Chemical composition of SWS-MCC

Sample	%Cellulose	%Hemicelluloses	%Lignin	%Yield
SWS-MCC	85.01 ± 1.22	3.03 ± 0.87	4.81 ± 1.74	58.0
Avicel PH 102	80.81 ± 1.14	5.10 ± 0.51	1.22 ± 0.97	-

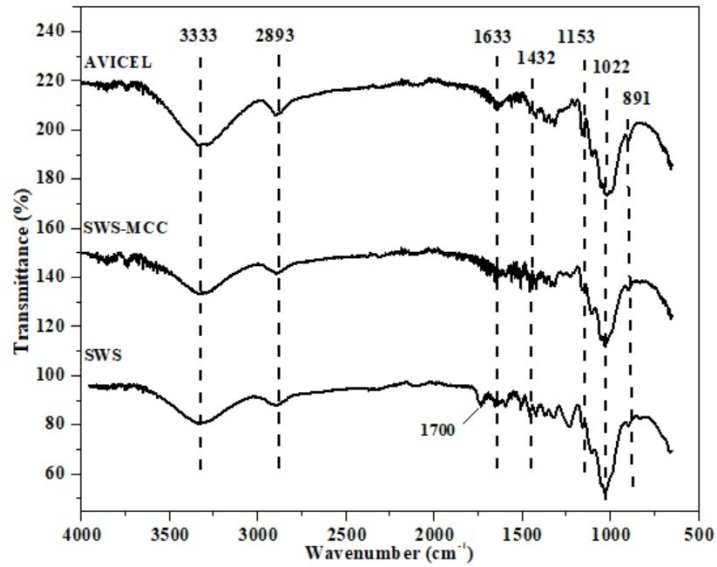


Figure 1: FT-IR spectra of SWS, SWS-MCC and Avicel

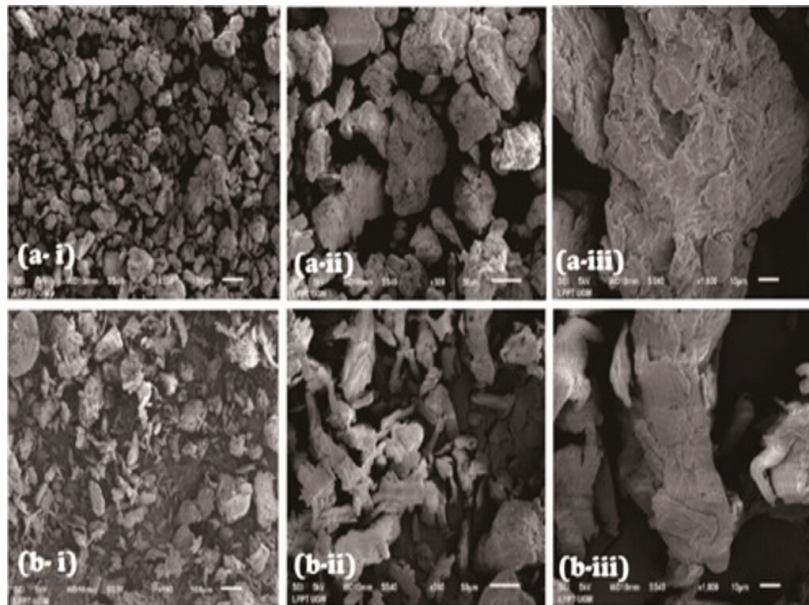


Figure 2: SEM micrographs of (a) SWS-MCC and (b) Avicel at (i) 100x, (ii) 300x, and (iii) 1000x magnifications

Morphological analysis (SEM)

SEM analysis aims to observe the surface characteristics of the resulting cellulose membrane. SEM micrographs of SWS-MCC and Avicel, for comparison, are shown in Figure 2. It was found that SWS-MCC showed a smooth surface, and no wax layer and non-cellulosic components were detected on the surface of the fiber, similar to other wood fibers.^{2,37} This shows that the delignification and hydrolysis processes can reduce most of the non-cellulosic components.

Figure 2 shows SWS-MCC and Avicel, with cross-sectional structures consisting of a highly dense layer and a porous layer. The large pore layer is caused by small damage to the pore walls, which combine to form pores of a larger size. This is also influenced by the process of solvent evaporation during the drying process. It can be seen that the size is not uniform in SWS-MCC because the cellulose has a very wide difference in the molecular weight range, as also seen in MCC from corncob^{28,18} and banana peel.³⁸ SWS-MCC appears to have a round or spherical morphology and is more granular than Avicel.

This occurs from the aggregation of multiple particles because water vapor is trapped in them. The resulting structure is similar to the morphology of cellulose found in Malaysian sago.³⁹

X-ray diffraction

The XRD patterns of SWS and SWS-MCC, as well as that of Avicel as a commercial comparison, are presented in Figure 3, to distinguish between the amorphous and the crystalline forms of MCC. It is seen that there is no peak related to semicrystalline cellulose in SWS-MCC due to the loss of amorphous properties, so what remains is α -cellulose.⁶ The XRD pattern of SWS shows a wide peak at $2\theta = \pm 20^\circ$ related to the amorphous polymer structure of hemicelluloses⁴⁰ and at $2\theta = 24.2^\circ$ related to crystalline carbon.⁴¹ The XRD pattern in Figure 3 reveals that in SWS and SWS-MCC, the presence of two peaks at $2\theta = 15.8^\circ$ and 22.6° is well identified, which shows that SWS-MCC is type cellulose I. The same results were also confirmed for cellulose from other raw materials.^{18,36,2} Besides, these two peaks, there is also one peak $2\theta = 34.6^\circ$ on SWS and SWS-MCC where the

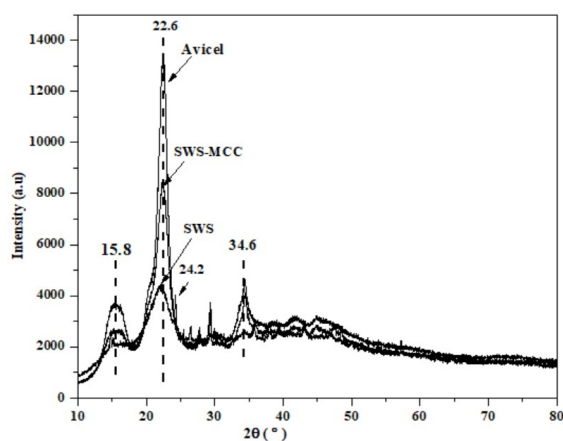


Figure 3: X-ray diffraction patterns of SWS, SWS-MCC and Avicel

Thermal analysis

The thermal properties and phase transitions of SWS-C and SWS-MCC were observed by DSC. From the DSC test results, the melting point temperature (T_m) and glass transition temperature (T_g) can be determined. T_g is an important property in polymers, at this temperature, the glassy state changes to the rubbery state. Figure 4 indicates that the T_g of SWS-C was 109.8°C , and

three peaks indicate that alkali delignification and acid hydrolysis treatments do not change the crystal structure of cellulose.⁶

As seen in Figure 3, in SWS, there is a peak at $2\theta = 24.2^\circ$. This shows that there are also other impurities that will be removed by the delignification treatment, as proven by SWS-MCC. Also, there is no double peak visible in the XRD pattern at $2\theta = 22^\circ$ - 24° , which indicates the presence of cellulose type I.⁴² Similar results were found in the XRD patterns of Avicel as a commercial comparator. The crystallinity index of SWS-MCC (33.8%) is greater than that of SWS (21.3%), as seen in the peak of the SWS-MCC XRD pattern at $2\theta = 22.6^\circ$, which looks sharper than in SWS. This shows an increase in the crystallinity index after the hydrolysis process. This increase occurs due to the loss of some of the amorphous cellulose through the hydrolysis process with HCl, which causes the hydrolytic bonds to break β -1,4-glucopyranose, so that individual crystallites of cellulose can be released.^{33,43} This increase in crystallinity can lead to increased mechanical properties in composites due to the higher tensile strength of the fibers.³³

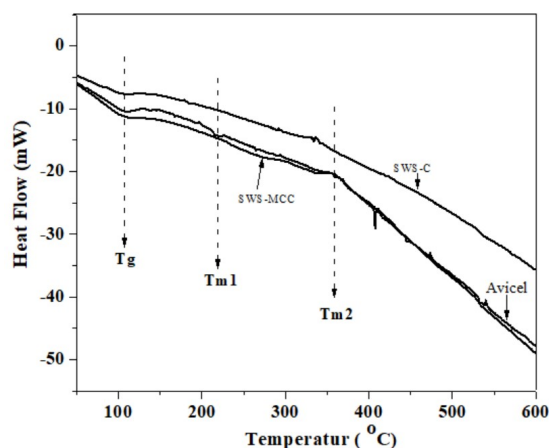


Figure 4: DSC thermograms of SWS-C, SWS-MCC and Avicel

there was a decrease in T_g in SWS-MCC (105.9°C). This shows that the influence of acid hydrolysis causes an increase in the flexibility of the polymer chain, so that the ability to move the atoms increases, as indicated by a decrease in the T_g of SWS-MCC.⁴⁴ The T_{m1} of SWS-C was detected at 189.8°C and there was an increase in the T_{m1} of SWS-MCC to 230.4°C (Fig. 4), which shows that hydrolysis does not cause damage to

the cellulose molecular chain.⁴⁵ The hydrolysis effect was also seen to increase T_{m2} in SWS-C (329.8 °C) and SWS-MCC (363.9 °C), where at a temperature of more than 300 °C degradation occurs.⁴⁶ As previously reported from DSC analysis, the thermal degradation temperature of cotton waste cellulose is in the range of 175-360 °C.⁴⁷ The DSC results (Fig. 4) show a negative value, which means that SWS-C, SWS-MCC and the commercial sample (Avicel) experienced an endothermic process that was visible starting at a temperature of 330 °C, with significant changes in heat flow.⁴⁸ The DSC thermogram of SWS-MCC (Fig. 4) also shows the presence of 3 (three) phases with different intensities, the first is visible to have low intensity at a temperature of around 160 °C, describing the evaporation of water.⁴⁹ Next, in the range of 230-300 °C, the degradation of the cellulose component occurs.⁴⁷ The third endothermic peak is around 360 °C, which is known to occur due to carbon residue destruction.⁵⁰ SWS-MCC tends to combine to form compact crystals when the amorphous part is lost in the acid hydrolysis process.^{47,51}

CONCLUSION

Microcrystalline cellulose was successfully prepared from Sengon wood sawdust. SEM micrographs show that SWS-MCC has a spherical shape, with a smooth and porous surface. The cellulose component was unchanged, and lignin was effectively removed from the fibers after the fabrication process, as evidenced by FTIR analysis. SWS-MCC has a crystallinity index of 33.8%, indicating cellulose type I structure. The DSC thermogram shows good thermal stability. From the findings of this research, it can be concluded that Sengon wood industrial waste can be used as a source of microcrystalline cellulose, a useful added value product, through three preparation stages, namely delignification, hydrolysis and bleaching, yielding a cellulose content of 85.01%. The analysis findings consistently show that SWS-MCC has similar characteristics to those of the commercial standard. Therefore, Sengon wood sawdust has the potential to become an alternative source for extraction of microcrystalline cellulose, thus addressing the issue of wood industry waste effectively.

ACKNOWLEDGEMENT: The authors would like to express their gratitude for The Indonesian

Education Scholarship Program (BPI) within the Indonesian Ministry of Education and Culture (Kemendikbud RI) funded by the Indonesian Endowment Fund for Education (LPDP).

REFERENCES

- H. Krisnawati, E. Varis, M. Kallio and M. Kanninen, “*Paraserianthes falcataria* (L.) Nielsen Ecology, Silviculture and Productivity”, CIFOR, Bogor, 2011
- P. Chuayplod and D. Aht-Ong, *J. Met. Mater. Miner.*, **28**, 106 (2018), <https://doi.org/10.14456/jmmm.2018.xx>
- R. A. Y. Kharismi, Sutriyo and H. Suryadi, *Young Pharm.*, **10**, s79 (2018), <https://doi.org/10.5530/jyp.2018.2s.15>
- S. Collazo-Bigliardi, R. Ortega-Toro and A. Chiralt Boix, *Carbohyd. Polym.*, **191**, 205 (2018), <https://doi.org/10.1016/j.carbpol.2018.03.022>
- N. Y. Abu-Thabit, A. A. Judeh, A. S. Hakeem, A. Ul-Hamid, Y. Umar *et al.*, *Int. J. Biol. Macromol.*, **155**, 730 (2020), <https://doi.org/10.1016/j.ijbiomac.2020.03.255>
- T. Zhao, Z. Chen, X. Lin, Z. Ren, B. Li *et al.*, *Carbohyd. Polym.*, **184**, 164 (2018), <https://doi.org/10.1016/j.carbpol.2017.12.024>
- D. Trache, M. H. Hussin, C. T. Hui Chuin, S. Sabar *et al.*, *Int. J. Biol. Macromol.*, **93**, 789 (2016), <https://doi.org/10.1016/j.ijbiomac.2016.09.056>
- S. Hartati, E. Sudarmonowati, Fatriasari, E. Hermiati, W. Dwianto *et al.*, *J. Ind. Wood Res.*, **1**, 103 (2010), <https://doi.org/10.51850/wrj.2010.1.2.103-107>
- D. Sartika, A. P. Firmansyah, I. Junais, I. W. Arnata, F. Fahma *et al.*, *Int. J. Biol. Macromol.*, **240**, 124327 (2023), <https://doi.org/10.1016/J.IJBIOMAC.2023.124327>
- F. Masoudzadeh, M. Jamshidi and M. Fasihi, *J. Build. Eng.*, **21**, 213 (2019), <https://doi.org/10.1016/J.JOBE.2018.10.020>
- H. Ren, Z. Xu, M. Gao, X. Xing, Z. Ling *et al.*, *Int. J. Biol. Macromol.*, **227**, 827 (2023), <https://doi.org/10.1016/j.ijbiomac.2022.12.198>
- J. Krivokapić, J. Ivanović, J. Djuriš, D. Medarević, Z. Potpara *et al.*, *Saudi Pharm. J.*, **28**, 710 (2020), <https://doi.org/10.1016/J.JSPS.2020.04.013>
- H. Dai, Y. Chen, L. Ma, Y. Zhang and B. Cui, *Int. J. Biol. Macromol.*, **191**, 129 (2021), <https://doi.org/10.1016/J.IJBIOMAC.2021.09.063>
- M. F. Mubarak, A. M. Zayed and H. A. Ahmed, *Ind. Crop. Prod.*, **182**, 114896 (2022), <https://doi.org/10.1016/J.INDCROP.2022.114896>
- W. A. Rahman, A. S. Ismail and N. A. Majid, in *Mat. Today Procs. 8th ICSST Conference*, Malaysia, September 7-8, 2021, pp. 4055-4060
- P. J. Sheskey, W. G. Cook and C. G. Cable, “Handbook of Pharmaceutical Excipients”, 8th ed., Pharmaceutical Press, Washington DC, 2017
- I. M. Cahyani, E. Lukitaningsih, A. Adhyatmika

- and T. N. S. Sulaiman, *Trop. J. Nat. Prod. Res.*, **6**, 1570 (2022), <https://doi.org/10.26538/TJNPR/V6I10.3>
- ¹⁸ A. F. Tarchoun, D. Trache and T. M. Klapötke, *Int. J. Biol. Macromol.*, **138**, 837 (2019), <https://doi.org/10.1016/j.ijbiomac.2019.07.176>
- ¹⁹ L. Pachau, R. S. Dutta, L. Hauzel, T. B. Devi and D. Deka, *Carbohydr. Polym.*, **206**, 336 (2019), <https://doi.org/10.1016/j.carbpol.2018.11.013>
- ²⁰ P. N. Trisant, I. Gunardi and Sumarno, *Macromol. Symp.*, **391**, 2000016 (2020), <https://doi.org/10.1002/MASY.202000016>
- ²¹ I. M. Cahyani, Adhyatmika, E. Lukitaningsih and T. N. S. Sulaiman, *Sci. Technol. Indones.*, **8**, 666 (2023), <https://doi.org/10.26554/sti.2023.8.4.666-674>
- ²² I. M. Cahyani, A. Adhyatmika, E. Lukitaningsih and T. N. S. Sulaiman, *Int. J. Pharm. Res. Appl.*, **9**, 551 (2024), <https://doi.org/10.35629/7781-0902551559>
- ²³ A. Chesson, *J. Sci. Food Agric.*, **32**, 745 (1981), <https://doi.org/10.1002/JSFA.2740320802>
- ²⁴ J. Baruah, R. C. Deka and E. Kalita, *Int. J. Biol. Macromol.*, **154**, 672 (2020), <https://doi.org/10.1016/j.ijbiomac.2020.03.158>
- ²⁵ F. Kallel, F. Bettaieb, R. Khiari, A. García, J. Bras *et al.*, *Ind. Crop. Prod.*, **87**, 287 (2016), <https://doi.org/10.1016/J.INDCROP.2016.04.060>
- ²⁶ G. Siqueira, J. Bras and A. Dufresne, *Polymers*, **2**, 728 (2010), <https://doi.org/10.3390/POLYM2040728>
- ²⁷ B. Debnath, P. Duarah and M. K. Purkait, *Int. J. Biol. Macromol.*, **244**, 125354 (2023), <https://doi.org/10.1016/J.IJBIOMAC.2023.125354>
- ²⁸ X. Shao, J. Wang, Z. Liu, N. Hu, M. Liu *et al.*, *Ind. Crop. Prod.*, **151**, 112457 (2020), <https://doi.org/10.1016/j.indcrop.2020.112457>
- ²⁹ E. Suryanto and M. I. R. Taroreh, *Molekul*, **17**, 165 (2022), <https://doi.org/10.20884/1.JM.2022.17.2.5179>
- ³⁰ Y. Liu, A. Liu, S. A. Ibrahim, H. Yang and W. Huang, *Int. J. Biol. Macromol.*, **111**, 717 (2018), <https://doi.org/10.1016/j.ijbiomac.2018.01.098>
- ³¹ S. Ventura-Cruz, N. Flores-Alamo and A. Tecante, *Int. J. Biol. Macromol.*, **155**, 324 (2020), <https://doi.org/10.1016/J.IJBIOMAC.2020.03.222>
- ³² L. K. Kian, N. Saba, M. Jawaid and H. Fouad, *Int. J. Biol. Macromol.*, **156**, 347 (2020), <https://doi.org/10.1016/j.ijbiomac.2020.04.015>
- ³³ M. K. M. Haafiz, S. J. Eichhorn, A. Hassan and M. Jawaid, *Carbohydr. Polym.*, **93**, 628 (2013), <https://doi.org/10.1016/j.carbpol.2013.01.035>
- ³⁴ M. Rashid, M. A. Gafur, M. K. Sharafat, H. Minami, M. A. J. Miah *et al.*, *Carbohydr. Polym.*, **170**, 72 (2017), <https://doi.org/10.1016/J.CARBPOL.2017.04.059>
- ³⁵ W. A. Rahman, S. F. A. Rajak and N. A. Majid, *Sci. Lett.*, **13**, 1 (2019), <https://doi.org/10.1016/J.MATPR.2022.06.071>
- ³⁶ N. H. A. Rahman, B. W. Chieng, N. A. Ibrahim and N. A. Rahman, *Polymers*, **9**, 1 (2017), <https://doi.org/10.3390/polym9110588>
- ³⁷ M. Jonoobi, A. Khazaecian, P. M. Tahir, S. S. Azry and K. Oksman, *Cellulose*, **18**, 1085 (2011), <https://doi.org/10.1007/S10570-011-9546-7/METRICS>
- ³⁸ P. L. Hariani, F. Riyanti and R. D. Asmara, *Molekul*, **11**, 135 (2016), <https://doi.org/10.20884/1.JM.2016.11.1.202>
- ³⁹ A. K. Veeramachineni, T. Sathasivam, S. Muniyandy, P. Janarthanan, S. J. Langford *et al.*, *Appl. Sci.*, **6**, 170 (2016), <https://doi.org/10.3390/APP6060170>
- ⁴⁰ P. D. Carà, M. Pagliaro, A. Elmekawy, D. R. Brown, P. Verschuren *et al.*, *Catal. Sci. Technol.*, **3**, 2057 (2013), <https://doi.org/10.1039/c3cy20838a>
- ⁴¹ I. Abed, M. Paraschiv, K. Loubar, F. Zagrouba and M. Tazerout, *BioResources*, **7**, 1200 (2012)
- ⁴² M. F. Zhang, Y. H. Qin, J. Y. Ma, L. Yang, Z. K. Wu *et al.*, *Ultrason. Sonochem.*, **31**, 404 (2016), <https://doi.org/10.1016/J.ULTSONCH.2016.01.027>
- ⁴³ Z. Wang, Z. Yao, J. Zhou and Y. Zhang, *Carbohydr. Polym.*, **157**, 945 (2017), <https://doi.org/https://doi.org/10.1016/j.carbpol.2016.10.044>
- ⁴⁴ H. Fahim, A. Motamedzadegan, R. Farahmandfar and N. G. Khaligh, *Int. J. Biol. Macromol.*, **232**, 123268 (2023), <https://doi.org/10.1016/J.IJBIOMAC.2023.123268>
- ⁴⁵ M. B. K. Niazi, Z. Jahan, S. S. Berg and Ø. W. Gregersen, *Carbohydr. Polym.*, **177**, 258 (2017), <https://doi.org/10.1016/J.CARBPOL.2017.08.125>
- ⁴⁶ M. Asad, N. Saba, A. Asiri, M. Jawaid, E. Indarti *et al.*, *Carbohydr. Polym.*, **191**, 103 (2018), <https://doi.org/10.1016/j.carbpol.2018.03.015>
- ⁴⁷ V. Chaparala, G. R. K. Sastry and P. P. Prasanthi, *Mater. Today Proc.*, 2214 (2023), <https://doi.org/10.1016/J.MATPR.2023.05.134>
- ⁴⁸ J. Kristanto, M. M. Azis and S. Purwono, *Helicon*, **7**, e07669 (2021), <https://doi.org/10.1016/J.HELIYON.2021.E07669>
- ⁴⁹ S. Bano and Y. S. Negi, *Carbohydr. Polym.*, **157**, 1041 (2017), <https://doi.org/10.1016/J.CARBPOL.2016.10.069>
- ⁵⁰ S. M. L. Rosa, N. Rehman, M. I. G. De Miranda, S. M. B. Nachtigall and C. I. D. Bica, *Carbohydr. Polym.*, **87**, 1131 (2012), <https://doi.org/10.1016/J.CARBPOL.2011.08.084>
- ⁵¹ S. Rashid and H. Dutta, *Ind. Crop. Prod.*, **154**, 112627 (2020), <https://doi.org/10.1016/J.INDCROP.2020.112627>